

Gravity wave dynamics observed by optical airglow imaging in the South American sector: a comparative study.

A. F. Medeiros (Universidade Federal de Campina Grande /DF/CCT, Brazil).

Tel/Fax: +55 (83) 310-1196; e-mail: afragoso@df.ufcg.edu.br (A. F. Medeiros)

H. Takahashi (Instituto Nacional de Pesquisas Espaciais (INPE), Brazil)

R.A. Buriti (Universidade Federal de Campina Grande /DF/CCT, Brazil)

K. M. Pinheiro (Universidade Federal de Campina Grande /DF/CCT, Brazil)

D. Gobbi (Instituto Nacional de Pesquisas Espaciais (INPE), Brazil)

Keywords: Gravity wave, airglow, imager, winds

Abstract

An all-sky CCD imager for the airglow OH, O₂ and OI (557.7 nm) emissions was operated at Cachoeira Paulista (CP), Brazil (23 S, 45 W), under collaboration with the Utah State University, USA, in a period of 1998-2000. Another all-sky imager, which belongs to Instituto Nacional de Pesquisas Espaciais, has been operated at São João do Cariri (Cariri), Brazil (7 S, 36 W) since October 2000. This same imager was installed at Boa Vista (BV), Brazil (2.8 N, 60 W), in the Amazon region, during the period of September-December, 2002, participating in the Conjugate Point Equatorial Experiment (COPEX) Campaign. The purpose of this work is to compare the wave parameters for these sites and also to compare with the work previous of Taylor et al. (1997) in Alcântara (2.3° S, 44.5° W). The Cariri data used were from September 2000 to August 2001.

1. Introduction

Short-period gravity waves with wavelength from few kilometers to a few hundred kilometers have been studied in recent years by using sensitive cooled-CCD imagers to observe mesospheric airglow layers (e.g., Taylor et al., 1995a; Nakamura et al., 2001;

Swenson and Liu, 1998; Yamada et al., 2001; Ejiri et al., 2001,2002; Smith et al., 2003; Shiokawa et al., 2003; Liu and Swenson, 2003). The airglow imaging technique provides a simple and useful method to investigate horizontal characteristics of atmospheric gravity waves and their temporal evolution in the upper mesosphere and lower thermosphere (MLT) region. Most of the airglow image measurements reported in the literature concern short-period (<1 hour) wave characteristics. These waves have been attributed to freely propagating or ducted short-period gravity waves (Walterscheid *et al.*, 1999, Isler *et al.*, 1997; Taylor *et al.*, 1987).

Nakamura *et al.*, (1999) analyzed 18 months of OH image data obtained in Shigaraki (35° N, 136° E), and extracted gravity wave components. They found a seasonal variation of the wave characteristics. For the waves with horizontal wavelength longer than 18 km, the propagation direction was eastward in summer and westward in winter. Walterscheid *et al.* (1999), from 9 months of airglow image observations in Adelaide (35° S, 138° E), concluded that many waves were thermally ducted. For the waves with horizontal wavelengths of a few tens of kilometers, the preferential propagation direction was poleward in summer and equatorward in winter. Hecht *et al.*, (2001) suggested that most of the waves observed during the summer solstice originated from the south or southeast of the observation site. The data used were obtained at Urbana (40° N, 88°W). Medeiros *et al.* (2003) found from the Cachoeira Paulista (22.7° S, 45.0° W) image data that the propagation direction of the bands showed a seasonal variation. In summer, the preferential propagation direction was towards southeast. In winter, it was towards the northwest.

Taylor et al. (1997) carried out in Alcântara (2.3° S, 44.5° W) (Here after AL) the first observation by airglow imager in South America Sector. After this work Medeiros et al. (2003, 2004a) obtained climatology for Cachoeira Paulista (23° S, 45° W) (Here after

CP). Medeiros (2004b) also determined the characteristics of gravity waves for São João do Cariri (7° S, 36° W) (Here after Cariri). This work will compare these previous works (in South America Sector) with other measurements realized recently. These measurements were obtained in Boa Vista (2.8° S, 60° W) (Here after BV). Figure 1 shows the four locations (AL, CP, BV and Cariri).

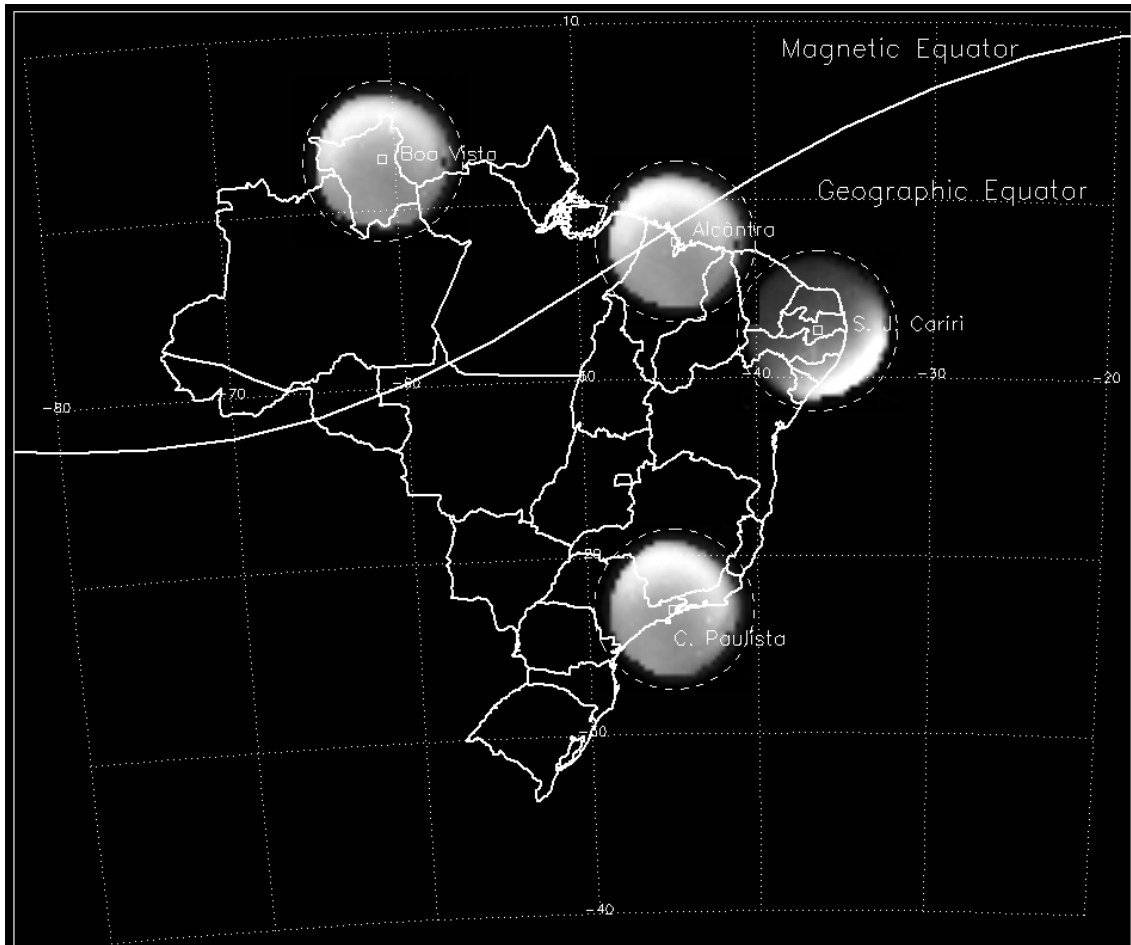


Figure 1 – Observations site

2. Observations

2.1 AL data

The imaging system was located at the Base de Lançamentos de Alcantra, Brazil, (2.3° S, 44.4° W). The measurements were in conjunction with the INPE/NASA Guara campaign during two observations periods; 6 August to 10 September, as part of the

MALTED program (Goldberg et al., 1995), and 1 to 16 October, as part of the SPREAD F program.

2.2 CP data

Airglow observations were carried out at CP using an all-sky imaging system. This was a collaborative program between the Instituto Nacional de Pesquisas Espaciais (INPE), Brazil and the Space Dynamics Laboratory, Utah State University (Dr. M. J. Taylor). The series of measurements were carried out over 12 consecutive months during October 1998 to September 1999.

2.3 Cariri data

An all-sky imager, which belongs to the INPE, has been operating at Cariri since October 2000. The Cariri data used were during September 2000 to August 2001.

2.4 BV data

This same all-sky imager that operated in Cariri was installed at BV, in the Amazon region, during the period of September-December, 2002, participating in the Conjugate Point Equatorial Experiment (COPEX) Campaign. The Table 1 shows a resume of the locations sites.

Table 1 – Site locations, observation period and geographic coordinates

Site	Observation Period	Geographic Coordinates
Alcântara (AL)	August-October/1994	(2.3 S, 44.5 W)
Cachoeira Paulista (CP)	October 1998 to September 1999	(23 S, 45 W)
São João do Cariri (Cariri)	September 2000 to August 2001	(7 S, 36 W)
Boa Vista (BV)	September-December/2002	(2.8 N, 60 W)

3. Results and Analyze

Figure 2 shows the distribution of horizontal wavelength as a function of their occurrence frequency for AL, CP, BV and Cariri. The data have been binned into of 5 km width. For AL the data exhibited a range extending ~10-45 km. It was detected 31 events during 3 months of observation. 10 of them (~32%) were concentrated between the interval of 15 and 20 km. The average wavelength was 24.3 km.

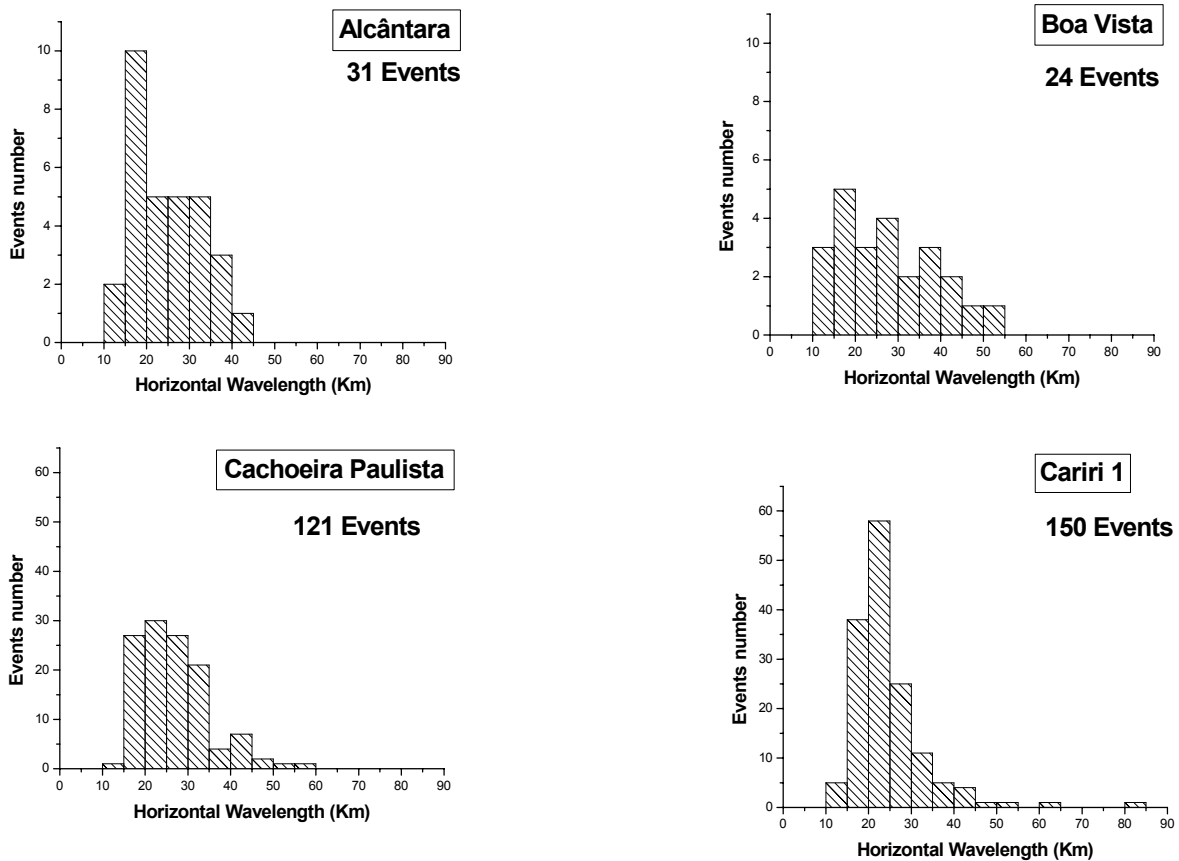


Figure 2 – Distribution of horizontal wavelength as a function of the occurrence frequency for the four sites.

For CP were detected 121 events during ~1 year of observation. The data exhibited a range extending ~10-60 but most of them were concentrated between 15 and 35 km. The average wavelength was 26.6 km. For BV the data exhibited a range extending ~10-55 km. It were detected 24 events during 4 months of observation. 50% of waves detected presented wavelength between 15 and 30 km. The average wavelength was

27.5 km. For Cariri the data, in a total of 150 events in 1 year of observation, exhibited a range extending practically between 10 and 55 km but wavelengths of ~ 60 and ~ 80 km were also observed. 80% of the events observed were concentrated between 15 and 30 km. The average wavelength was 24.7 km. Summarizing the range of observed wavelength for the four sites presented a good agreement but the distributions are different for every sites analyzed.

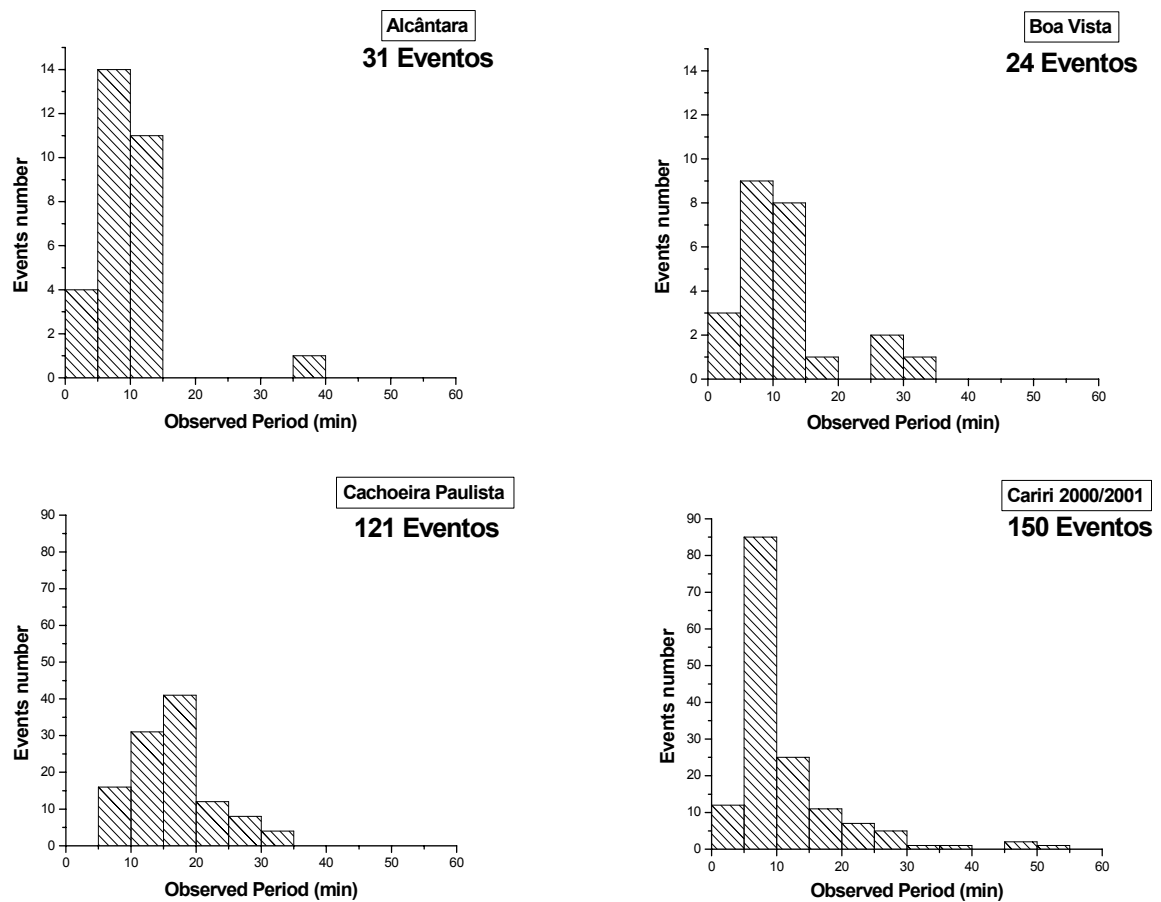


Figure 3 – Distribution of observed period as a function of the occurrence frequency for the four sites.

The Figure 3 shows histograms of the frequency of occurrence against wave period (binned into 5-minute intervals) for AL, CP, BV and Cariri. A clear difference can be seen between the CP and AL, BV and Cariri data. The histogram for CP, *e.g.* shows a somewhat wide range of period, approximately 90% of band events exhibiting periods

between 10 and 20 minutes. The average observed wave period was 16.6 min. On the other hand the histograms for AL, BV and Cariri shows a narrow range of distribution between 5 and 15 minutes. The highest frequency of occurrence occurs in the range of 5 to 10 minutes. The average waves periods were 9.6, 11.5 and 10.9 minutes for AL, BV and Cariri respectively. Some comments could be made about the distribution of frequency. Cariri presented almost 57% of wave detected between 5 and 10 minutes. It means that there is a strong concentration of waves occurrence with small periods but large periods can be observed also. On the other hand, AL presented 84% of the events with period between 5 and 15 minutes besides this there is “vacuum” of events not detected between 15 and 35 minutes. BV presented 71% of the events with period between 5 and 15 minutes.

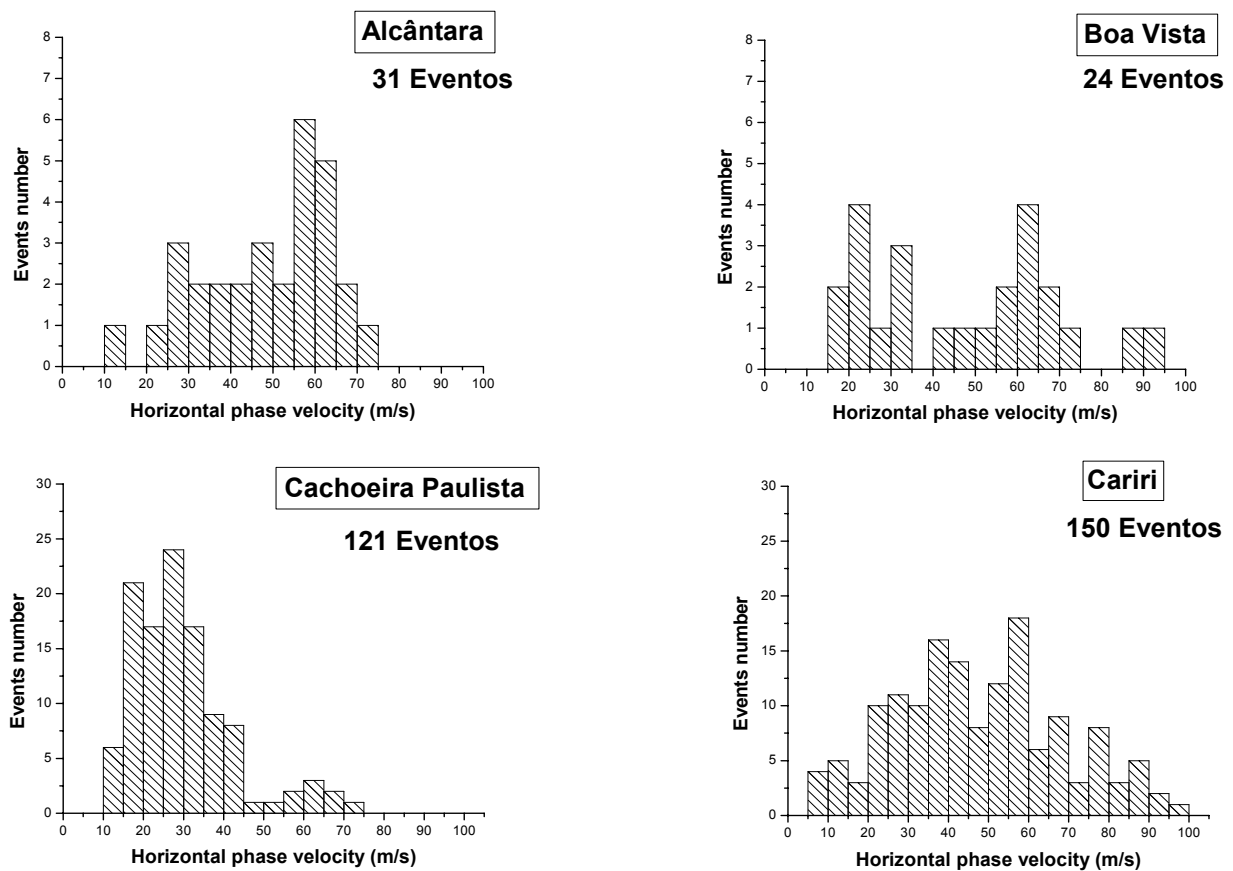


Figure 4 – Distribution of phase velocity as a function of the occurrence frequency for the four sites.

The difference in the wave characteristics among the sites becomes apparent when we look into the histograms of the phase speed distributions. Figure 4 shows the distribution of phase speed plotted in 10 m/s intervals for AL, CP, BV and Cariri. The phase speed at CP is concentrated in a range of 10 to 40 m/s, with an average of 29.6 m/s. At AL, BV and Cariri, on the other hand, the average phase velocities were 48.0, 47.6 and 48.9 m/s for AL, BV and Cariri respectively. Clearly, the phase velocities at AL, BV and Cariri are higher than at CP. But, in AL and BV, the velocity distribution is spreading differently from CP and Cariri where we can define a peak of velocity. Further on we will argue this question.

The wave propagation directions are summarized in Figure 5. The frequency of occurrence diagrams are binned in 15° intervals.

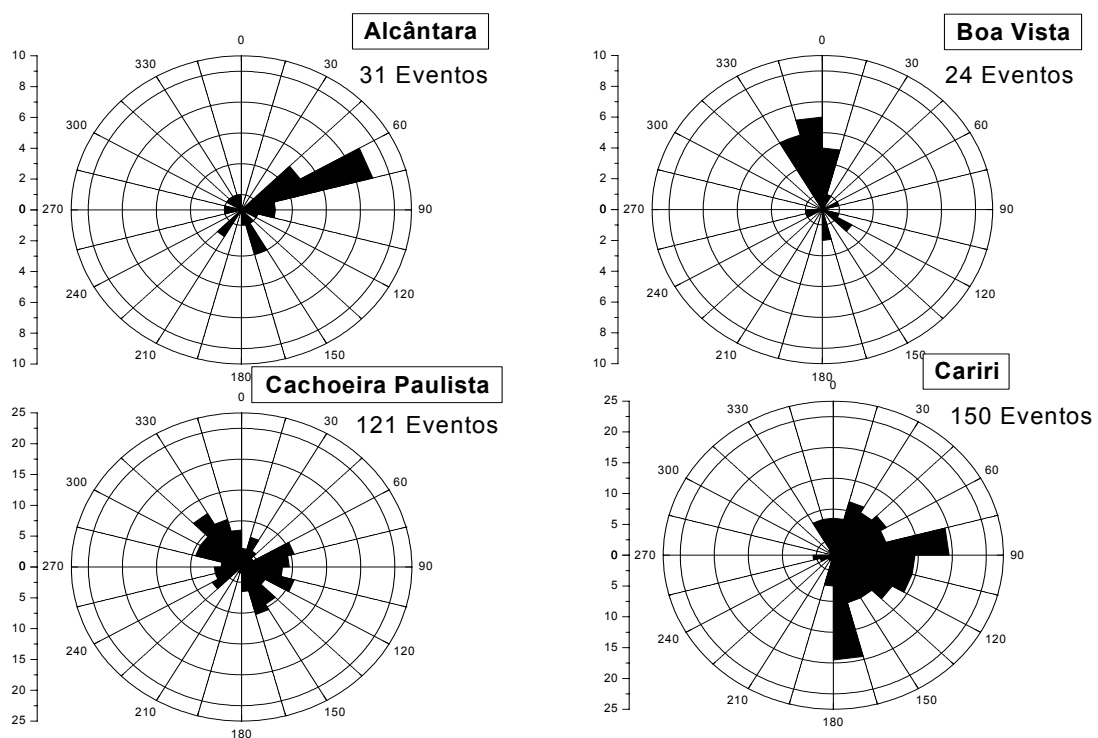


Figure 5 - Frequency of occurrence of the propagation direction of the gravity waves observed at Al, CP, BV and Cariri.

The distribution for AL presented a preferential direction to northeast (azimuth range 0°-90°). From 31 events, 12 moved between 45 and 75 degrees. It represents ~39%.

Adding to this information, 21 events have component moving from west to east. This direction is from continent to sea. The distribution of the CP data is highly anisotropic, exhibiting two directions of preference: southeast (azimuth range 90° - 180°), from continent to ocean, and northwest (azimuth range 270° - 360°). At BV this direction preferential is to north, also, from continent to sea. From 24 events, 17(it is equivalent to $\sim 71\%$) have component moving from south to north. The south of BV is located the Amazon Florest where the production of water vapor, clouds and convection is strong. The Cariri data show a preferential wave propagation direction to east (from the continent to the ocean). From a total of 150 bands observed, 131 events (87.3%) showed a propagation direction towards the east.

In order to examine the seasonal tendency of the wave parameters, the data were grouped in four seasons: summer (November, December, January and February), autumn (March and April), winter (May, June, July and August) and spring (September and October). No clear seasonal variation was found with respect to wavelength, period or phase velocity at either observation site. However, the propagation direction did show a clear seasonal dependency. However, CP during the summer the preferential propagation direction is southeastward. In winter it changed towards northwest. No clear preferential propagation direction was observed during the Spring and Fall equinox. In the case of Cariri, the preferential propagation direction is towards southeast during the summer and northeast during the winter (Medeiros et al., 2004).

4. Discussion

The band-type gravity waves in the mesopause region, observed by airglow imagers located in four different latitude regions, showed different features in their wave characteristics. The phase velocities for the AL, BV and Cariri data exhibited higer

values than CP. The anisotropy of the wave propagation direction also shows some differences between the four sites.

The wave propagation direction in the mesopause region depends on two factors, its source location in the lower atmosphere, relative to the observer, and the background wind field below the observation layer. Gravity waves propagating upward from the lower atmosphere are absorbed into the mean flow as they approach a critical layer where the intrinsic frequency of the wave is Doppler-shifted to zero. This situation may occur at any height when the local horizontal wind speed along the direction of propagation equals the apparent horizontal phase speed of the gravity wave. Gravity waves with horizontal phase velocities outside of this region would not meet, by chance, a critical layer and should be observable. The anisotropy of the wave propagation direction observed mainly in summer and winter at CP and Cariri could be due to seasonal variation of the stratospheric and mesospheric wind fields (Medeiros et al., 2004). The gravity wave activities over the four sites could be related also to the tropospheric convection because the propagation direction at all sites are from Continent to Sea.

It should be emphasized that we find the apparent phase velocities at AL, BV and Cariri to be higher than those at CP. Nakamura *et al.* (2002) also found a higher phase velocity at Jakarta (6.9°S, 107.9°E) and suggested that this could be due to weak wind velocity in the equatorial region. The weak winds generate minor blocking because the blocking diagrams depends of the wind velocity (Medeiros et al., 2004). However, it is too early to conclude that the difference in the observed phase speed is mainly due to the Doppler effect. Figure 6 shows the average phase velocities by the four locations.

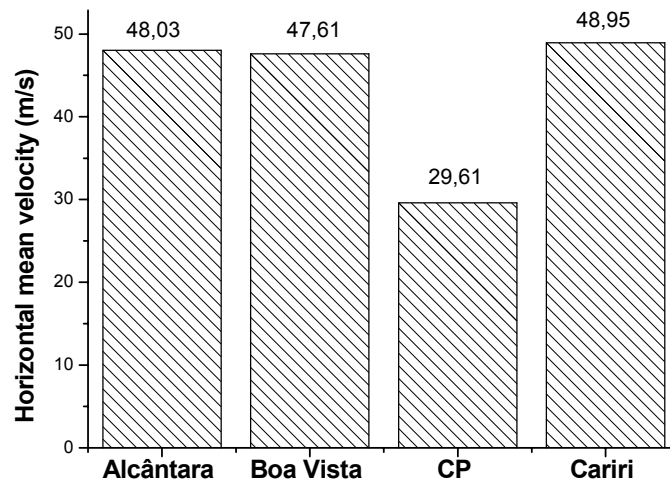


Figure 6 – Average phase velocities by the four sites

Since the data sets at AL, CP, BV and Cariri are only one year in length, and do not overlap, it is possible that the differences between the waves observed at the two sites are due to interannual variability. Further measurements are needed before any conclusion can be drawn.

5. Conclusion

The band-type gravity waves in the mesopause region, observed by airglow imagers located in four different latitude regions, showed different features in their wave characteristics. The phase velocities for the AL, BV and Cariri data exhibited higher values than CP. The anisotropy of the wave propagation direction also shows some differences between the four sites. The gravity wave activities over the four sites could be related to the tropospheric convection because the propagation direction at all sites are from Continent to Sea. The anisotropy of the wave propagation direction observed mainly in summer and winter at all sites could be due to seasonal variation of the stratospheric and mesospheric wind fields. The apparent phase velocities at Cariri, AL and BV are higher than at CP which can be attributed to weak wind at equatorial region. Since the data set at four sites are each one year length and are non overlapping, it is possible that the differences between the measurements at four sites are due to interannual variability. Together, these observations suggest that different sources also could be responsible by the distinctive results.

Acknowledgments

The Cariri imager was financed by CNPq/PRONEX grant No. 76.97.1079.00, and the USU camera and operations were supported by NSF grant No. ATM-9525815. This work has also been supported by the Fundação de Amparo à Pesquisa do Estado de São Paulo and CNPQ. The authors are also grateful to São João do Cariri Prefecture for technical support.

References

- Ejiri, M. K., K. Shiokawa, T. Ogawa, M. Kubota, T. Nakamura, and T. Tsuda, 2002, Dual-site imaging observations of small-scale wave structures through OH and OI nightglow emissions, *Geophys. Res. Lett.*, 29(10), 1445.
- Ejiri, M. K., K. Shiokawa, T. Ogawa, T. Nakamura, R. Maekawa, T. Tsuda, and M. Kubota, 2001 Observations of small-scale gravity waves near the mesopause obtained from four all-sky CCD imagers and the MU radar, *J. Geophys. Res.*, 106, 22,793–22,799.
- Isler J. R., Taylor M. J., and Fritts D. J., 1997. Observational evidence of wave ducting and evanescence in the mesosphere, *J. Geophys. Res.*, 102, 26301-26313.
- Liu, A. Z., and G. R. Swenson, 2003, A modeling study of O₂ and OH airglow perturbations induced by atmospheric gravity waves, *J. Geophys. Res.*, 108(D4), 4151.
- Medeiros, A. F.; Buriti, R. A.; Machado, E. A; Taylor, M. J.; Takahashi, H.; Batista, P. P.; Gobbi, D. 2004, Comparison of Gravity Wave Activity Observed by airglow imaging from two different latitudes in Brazil. *Journal of Atmospheric And Solar-Terrestrial Physics*, v. 66/6-9, p. 647-655.
- Medeiros, A. F.; Takahashi, H.; Batista, P. P.; Gobi, D.; Taylor, 2004, M. Observation Of Atmospheric Gravity Waves Using Airglow All-Sky Ccd Imager at Cachoeira Paulista (23 ° S, 45 ° W). *Geofísica Internacional*, V. 43, N. 1, P. 29-39.

- Medeiros, A. F.; Taylor, M. J.; Takahashi, H.; Batista, P. P.; Gobi, D., 2003. An Investigation of gravity wave activity in the low-latitude upper mesosphere: propagation direction and wind filtering, *J. Geophys. Res.*, 108(D14), 4411-4419.
- Nakamura T., Higashikawa A., Tsuda T., and Matsushita Y., 1999. Seasonal variations of gravity wave structures in OH airglow with a CCD imager at Shigaraki, *Earth Planets Space*, 51, 897-906.
- Nakamura, T., T. Tsuda, R. Maekawa, M. Tsutsumi, K. Shiokawa, and T. Ogawa, 2001, Seasonal variation of gravity waves with various temporal and horizontal scales in the MLT region observed with radar and airglow imaging, *Adv. Space Res.*, 27, 1737– 1742.
- Nakamura, T.; Aono, T.; Tsuda, T.; Martimungum, D. R. and Achmad, E. 2002. Mesospheric gravity waves over tropical convective region observed by OH airglow imaging in Indonesia, THIRD PSMOS INTERNATIONAL SYMPOSIUM ON DYNAMICS AND CHEMISTRY OF THE MLT REGION, Foz do Iguacu Planetary Scale Mesopause Observing System.
- Shiokawa, K., M. K. Ejiri, T. Ogawa, Y. Yamada, H. Fukunishi, K. Igarashi, and T. Nakamura, 2003, A localized structure in OH airglow images near the mesopause region, *J. Geophys. Res.*, 108(D2), 4048.
- Swenson, G. R., and C. S. Gardner, 1998 Analytical models for the responses of the mesospheric OH* and Na layers to atmospheric gravity waves, *J. Geophys. Res.*, 103, 6271–6294.
- Swenson, G. R.; Haque, R.; Yang, W.; Gardner, C. S., 1999. Momentum and energy fluxes of monochromatic gravity waves observed by an OH imager at Starfire Optical Range, New Mexico *J. Geophys. Res.* 104,D6, 6067-6080.

- Taylor M. J. and M. A. Hapgood, 1990. On the origin of ripple-type wave structure in the nightglow emission, *Planet. Space Sci.*, 38, 1421-1430.
- Taylor M. J., and Hapgood M. A., 1988. Identification of a thunderstorm as a source of short period gravity waves in the upper atmospheric nightglow emission, *Planet. Space Sci.*, 36, 975-985.
- Taylor M. J., Hapgood M. A., and Rothwell P., 1987. Observations of gravity wave propagation in the OI (557.7 nm), Na (589.2 nm) and the near infrared OH nightglow emissions, *Planet. Space Sci.*, 35, 413-427.
- Taylor M. J., Ryan E. H., Tuan T. F., and Edwards R., 1993. Evidence of preferential directions for gravity wave propagation due to wind filtering in the middle atmosphere, *J. Geophys. Res.*, 98(A4), 6047-6057.
- Taylor, M. J.; Pendleton, W. R., Jr; Clark, S.; Takahashi, H. Gobbi, D.; Goldberg, R. A., 1997. Image measurements of short-period gravity waves at equatorial latitudes. *J. Geophys. Res.*, 102, D22, 26,283-299.
- Walterscheid R. L., Hecht J. H., Vincent R. A., Reid I. M., Woithe J., and Hickey M. P., 1999. Analysis and interpretation of airglow and radar observations of quasi-monochromatic gravity waves in the upper mesosphere and lower thermosphere over Adelaide, Australia (35° S, 138°). *Journal of Atmos. Sol. Terr. Phys.*, 61, 461-468.